Modification of the Distal Histidyl Imidazole in Myoglobin to *N*-Tetrazole-Substituted Imidazole and Its Effects on the Heme Environmental Structure and Ligand Binding Properties

Shin-ichi Adachi[‡] and Isao Morishima*

Division of Molecular Engineering, Graduate School of Engineering, Kyoto University, Kyoto 606-01, Japan

Received March 11, 1992; Revised Manuscript Received June 17, 1992

ABSTRACT: The mechanism of *N*-tetrazole ring formation at the distal histidyl imidazole of sperm whale myoglobin (Mb) has been studied by nitrogen-15 (^{15}N) NMR spectroscopy by utilizing ^{15}N-labeled cyanogen bromide (BrCN) and azide ion (N_3^-). The ^{15}N-NMR spectrum of Br$C^{15}N$-modified Mb + N_3^- afforded two hyperfine-shifted ^{15}N resonances, both of which are identical with the resonance positions of two of the three ^{15}N resonances for BrCN-modified Mb + $^{15}NN_2^-$. This unusual spectral feature is due to the formation of the *N*-tetrazole ring attached to the distal histidyl imidazole and the scrambling of the labeled nitrogen originated from N_3^- or BrCN over the tetrazole ring upon coordination to the ferric heme iron. The ferric iron-bound *N*-tetrazole ring comes off upon reduction to the ferrous state, and the stable CO complex of tetrazole-modified Mb (tetrazole-Mb) is formed. Electronic absorption and ^1H-NMR spectra of deoxy and carbonmonoxy forms of tetrazole-Mb are slightly altered from those of native Mb by the modification, while the most significant effect is exerted on the C–O stretching frequency of iron-bound CO. The C–O stretching band for tetrazole-MbCO is observed at 1966 cm^{-1} in contrast to 1945 cm^{-1} for native MbCO, suggesting that the geometry of iron-bound CO in tetrazole-Mb is relatively upright which is characteristic of the "open" conformer. This result corresponds to the 15-fold increase of the CO association rate constant by the *N*-tetrazole modification of the distal His. The oxy form of tetrazole-Mb is readily autoxidized to its ferric state, indicating that hydrogen bonding between the distal His and iron-bound oxygen is essential for stable O_2 binding to the heme iron.

Great importance for the formation of the stable iron–oxygen complex in myoglobin (Mb)[1] has been ascribed to the distal histidine (His), which is located closely enough to interact with the iron-bound oxygen molecule. In fact, the neutron diffraction study of oxy-Mb (Phillips & Schoenborn, 1981) afforded evidence for the hydrogen bonding between the distal His and the coordinated oxygen. Further support for this view was provided by sperm whale Mb mutants in which the distal His is substituted by other amino acid residues by site-directed mutagenesis (Springer et al., 1989; Rohlfs et al., 1990; Carver et al., 1990). The expression of the sperm whale Mb gene in *Escherichia coli* has provided useful materials for probing the functional role of the highly conserved distal His. Substitution of the distal His always caused a decrease in O_2 affinity (Springer et al., 1989; Rohlfs et al., 1990), which is consistent with the idea that the hydrogen bond between the distal His and iron-bound O_2 lowers the free energy of O_2 binding by 1–2 kcal/mol.

On the other hand, we have been interested in facile and site-specific ways to modify the distal His of Mb, that is, chemical modification of the distal His (Shiro & Morishima, 1984; Morishima et al., 1985, 1989; Hori et al., 1989). Although it is difficult to introduce diverse functional groups as site-directed mutagenesis can do by utilizing chemical modification, this method has an advantage in introducing functional groups other than natural amino acid residues very easily. Chemical modification of Mb by a stoichiometric amount of cyanogen bromide (BrCN) afforded a BrCN-modified Mb (BrCN-Mb) in which the ϵ-nitrogen of the distal histidyl imidazole is N-cyanated (Jajczay, 1970; Shiro & Morishima, 1984). Further, an addition of azide ion (N_3^-) to BrCN-Mb afforded a ferric low-spin complex which was assigned in our previous paper to the simple BrCN-MbN_3^- complex (Shiro & Morishima, 1984). However, we noticed later that this complex did not give the azide IR bands in the 2000–2100-cm^{-1} region frequently encountered for the azide complex of native Mb (McCoy & Caughey, 1970), and the kinetic studies of the azide binding to BrCN-Mb exhibited an almost zero dissociation rate constant of azide. These unusual results allowed us to expect that the exogenous azide ligand could react with BrCN-Mb to form a stable novel complex of ferric Mb. Single-crystal EPR measurements suggested that this complex was not a simple BrCN-MbN_3^- complex but a novel Mb complex in which the *N*-cyano group would react with N_3^- to form an *N*-tetrazole-substituted His and that the tetrazole group might coordinate to the heme iron (Hori et al., 1989). This proposed structure of the novel Mb derivative with the *N*-tetrazole group attached to the distal histidyl imidazole (tetrazole-Mb) was later confirmed by the X-ray structural study (Kamiya et al., 1991). Such a novel and unique feature of the modified Mb prompted us to characterize its structure and the reaction mechanism to form the *N*-tetrazole ring attached to the distal histidine of Mb on the basis of the ^{15}N-NMR using ^{15}N-enriched azide and BrCN. In this report, we describe the identification of this novel compound formed by the specific modification of the distal histidine in Mb and show how this modification affects the heme environmental structure and the ligand binding properties.

* Correspondence should be addressed to this author.

‡ Present address: Photon Factory, National Laboratory for High Energy Physics, Tsukuba, Ibaraki 305, Japan.

[1] Abbreviations: Mb, myoglobin; MbCO, carbonmonoxymyoglobin; BrCN-Mb, chemically modified myoglobin with an *N*-cyano group at the distal histidyl imidazole; tetrazole-Mb, chemically modified myoglobin with an *N*-tetrazole group at the distal histidyl imidazole.

0006-2960/92/0431-8613$03.00/0

EXPERIMENTAL PROCEDURES

Sperm whale myoglobin (type II) was obtained from Sigma. Singly and doubly ^{15}N-labeled azide (i.e., $^{15}N{=}N{=}N^-$ and $^{15}N{=}^{15}N{=}N^-$, respectively) and ^{15}N-labeled BrCN ($BrC^{15}N$) were purchased from Cambridge Isotope Laboratories, Co., and nonenriched NaN_3 and BrCN were from Wako Pure Chemical Industries, Ltd. The reaction of Mb with BrCN was performed by the method described previously, that is, addition of a stoichiometric amount of BrCN to met-Mb in 0.1 M potassium phosphate buffer at pH 7 (Jajczay, 1970; Shiro & Morishima, 1984; Morishima et al., 1989). To convert the *N*-cyano group of the distal histidyl imidazole to the *N*-tetrazole, a 1.5–10-fold excess of N_3^- was simply added to the BrCN-Mb solution. The reaction of BrCN-Mb with N_3^- was monitored by a Hitachi U-3210 UV–visible spectrophotometer. The time course of the reaction showed uniform changes with isosbestic points throughout the course of reaction, which indicates the homogeneity of the product. All chemicals were used without further purification. Unless specially stated, 0.1 M KPB, pH 7.0, was used as the buffer solution.

^{15}N- and ^1H-NMR spectra were recorded at 30 and 300 MHz, respectively, on a Nicolet NT-300 spectrometer equipped with a 1280 computer system. In order to measure ^{15}N-NMR spectra, typically 800 000–1 000,000 transients were accumulated with a sweep width of 20 000 Hz. The intensity of the ^{15}N-NMR signals was determined by the usual integration method. For recording of the paramagnetically shifted proton NMR spectra, typically 10 000–30 000 transients were accumulated to obtain the Fourier-transformed spectra with 4K data points and a 6.2-ms 90° pulse. For the measurement of diamagnetic species such as the CO form of Mb, 1000 transients were accumulated with 16K data ponts and a 1-s delay time. The UV–visible absorption spectra were recorded with a Hitachi U-3210 UV–visible spectrophotometer by using a cell with a 1-cm path length.

The infrared spectra of MbCO were recorded on a Nicolet 20 DXB FT-IR spectrometer. A total of 500 transients with a resolution 0.5 cm^{-1} was accumulated to yield the resultant spectra. The CaF_2 IR cell with a 0.025-mm path length was used.

CO association rates (k_{on}) of Mb's were measured by a laser flash photolysis method as reported previously (Adachi & Morishima, 1989). Samples for photolysis measurements were prepared immediately prior to use. Concentrated solutions of the ferric forms of proteins were diluted to an absorbance at 409 nm of approximately 1.5. The solutions were equilibrated with CO up to 1 atm (101 325 Pa) and then reduced by the addition of a small amount of dithionite. For the micro- and millisecond laser photolysis experiments, a flash lamp pumped dye laser with a half duration of 300 ns (UNISOKU LA-501) was used. Rhodamine 6G (Kodak) in methanol was used to produce an excitation flash at a wavelength of 590 nm. A Xe flashlamp was used to probe the sample absorbance. The probe light was focused onto the slit of a monochromator (UNISOKU USP-501) and detected by a photomultiplier. A transient memory (Graphtec TMR-80) was used to digitize the signal (50 ns/point max, 4096 points) and NEC PC-9801VX computer for further analysis. The bimolecular recombination was followed by monitoring the transient absorbance changes at 435 nm. Under the conditions of our experiment, the observed rate of recombination is pseudo-first-order in the concentration of deoxy-Mb, and pseudo-first-order rate constants were obtained from a nonlinear least-squares fit of the data to a single exponential. Activation energies for CO binding were obtained from the temperature dependence of (5–30 °C) of the CO association rate constants. A CO dissociation rate constant of tetrazole-Mb was determined by mixing the CO derivative in the presence of free CO at a low concentration with a high concentration of potassium ferricyanide (1 mM). It was assumed that potassium ferricyanide only reacted with the unliganded Mb formed by dissociation of the CO derivative.

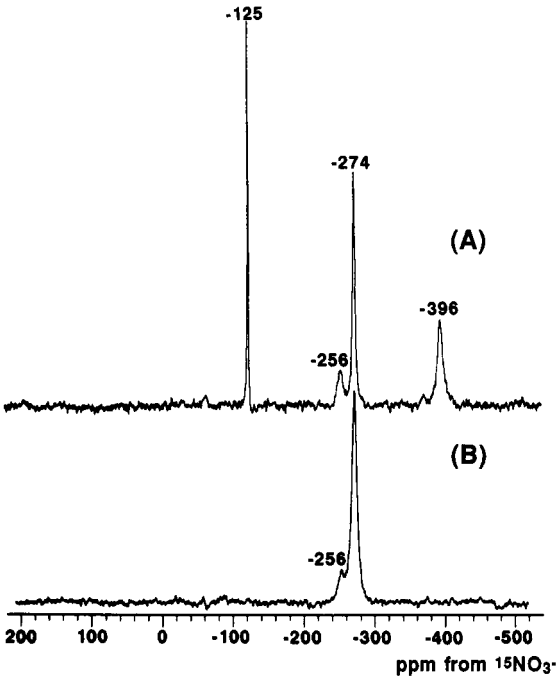

FIGURE 1: ^{15}N-NMR spectra (at 30.4 MHz, $^{15}NO_3^-$ as an external reference) of (A) doubly and (B) singly ^{15}N-labeled azide complexes of native Mb at pH 7 and 23 °C. Two sharp signals correspond to bulk free azide ion (–125 ppm for central ^{15}N and –274 ppm for terminal ^{15}N). An additional signal observed at –256 ppm arises from peptide ^{15}N (natural abundance).

RESULTS

Mechanism of N-Tetrazole Ring Formation Revealed by ^{15}N-NMR Spectroscopy. ^{15}N-NMR spectra of doubly and singly ^{15}N-labeled azide complexes of native Mb are shown in Figure 1. In the spectrum of native $Mb^{15}N_2N$ (Figure 1A), one hyperfine-shifted signal is observed at –396 ppm, with a concomitant appearance of bulk free $^{15}N_2N^-$ signals at –125 (central) and –274 ppm (terminal) and a peptide ^{15}N signal (natural abundance) at –256 ppm (Witanowski et al., 1981). In the case of native $Mb^{15}NN_2$ (Figure 1B), no iron-bound ^{15}N signal of azide is observed, and it is likely that the ^{15}N resonance of the iron-bound nitrogen is broadened out, and the ^{15}N resonance of the terminal nitrogen of azide is also broadened out because of the exchange of the iron-bound azide.

The ^{15}N-NMR spectra of the reaction products of BrCN-Mb with doubly and singly ^{15}N-labeled azide and of $BrC^{15}N$-Mb with nonlabeled azide are shown in Figure 2. Patterns of signals in these spectra were significantly different from those in the native Mb's spectra. It is quite interesting to note that three hyperfine-shifted ^{15}N resonances with 1:3:1 relative intensities are observed at 45, –106, and –366 ppm for BrCN-Mb + $^{15}N_2N$ (Figure 2A) and that BrCN-Mb + $^{15}NN_2$ affords the same resonances with equal intensities (Figure 2B). It is also surprising that $BrC^{15}N$-Mb + N_3 exhibits the 45 and –366 ppm resonances with 1:1 intensities, identical with two of the three peaks observed for the reaction products of BrCN-Mb with ^{15}N-enriched azide (Figure 2C). These unusual

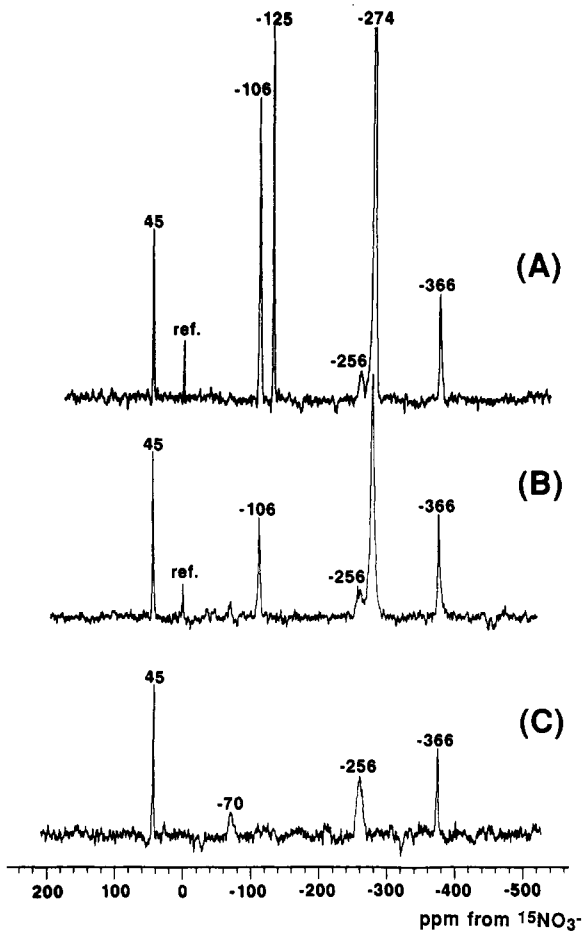

FIGURE 2: ^{15}N-NMR spectra of (A) doubly and (B) singly ^{15}N-labeled azide complexes of BrCN-Mb and (C) nonlabeled azide complex of BrC^{15}N-Mb at pH 7 and 23 °C. A signal originated from bulk free BrC^{15}N is also observed at −70 ppm in (C).

features of the ^{15}N-NMR spectra are reasonably explained by the structure in which the tetrazole ring attached to the distal histidyl imidazole is coordinated to the ferric heme iron (Figure 3). First of all, we assume that the *N*-cyano group of BrCN-Mb reacts with N_3^- to form an N-tetrazolated compound by 1,3-cycloaddition, followed by the binding of the nitrogen atom of the *N*-tetrazole ring to the heme iron. The tetrazole ring is symmetrical with respect to the bond between the distal histidyl imidazole and the tetrazole ring, which allows two rotational isomers of the tetrazole ring. This reaction mechanism allows us to see a scrambling of the labeled nitrogen(s) originated from N_3^- or BrCN over a tetrazole ring and enables us to assign the ^{15}N-NMR signals in Figure 2.

When BrCN-Mb reacts with singly ^{15}N-labeled azide (^{15}N=N=N$^-$), the labeled nitrogen is to be placed either at the position of N(2) or N(4) in the *N*-tetrazole ring (Figure 3). Upon coordination of this ^{15}N-labeled tetrazole to the ferric heme iron in the two binding modes, the labeled nitrogen should be located at N(1), N(2), N(3), and N(4) with equal intensities. The observed ^{15}N-NMR spectrum in Figure 2 is thus reasonably explained, if we assume that the ^{15}N resonance of the iron-bound nitrogen (N(2) in Figure 5B) is broadened out due to the proximity effet of the paramagnetic iron atom. When the doubly ^{15}N-labeled azide reacts with BrCN-Mb to form an *N*-tetrazole ring bound to the heme iron, there are four possible conformers with the two ^{15}N-labeled nitrogens located for each conformer at the 2 and 3, 3 and 4, 1 and 2, and 2 and 3 positions, leading to three ^{15}N peaks for the ^{15}N-(4), ^{15}N(3), and ^{15}N(1) nitrogens with 1:3:1 relative intensities, respectively, and one broadened out signal for the ^{15}N(2) nitrogen with 3-fold intensities. This spectral analysis allows us to assign unambiguously the 45, −106, and −366 ppm resonances to the ^{15}N(4), ^{15}N(3), and ^{15}N(1) nitrogens, respectively. The two ^{15}N peaks at 45 and −366 ppm for the BrC^{15}N-Mb + N_3^- system can be likewise interpreted; the ^{15}N-labeled nitrogen is located at N(1) and N(4) when the tetrazole ring is bound to the iron.

Characterization of Ferrous Derivatives of Tetrazole-Mb. When the tetrazole-Mb was reduced by the addition of dithionite, the deoxy form was obtained as confirmed by ^{1}H-NMR spectroscopies. The ^{1}H-NMR spectrum of deoxy-tetrazole-Mb is compared with that of native deoxy-Mb in Figure 4. An exchangeable proton signal at 81.7 ppm in Figure 4A corresponds to the proximal His N_δH which is located at 73.4 ppm for the native deoxy-Mb, implying that the tetrazole ring comes off from the heme iron upon reduction to make a five-coordinated deoxy form of tetrazole-Mb. Since the oxy form of tetrazole-Mb was susceptible to autoxidation, we could not detect a stable oxy complex. However, carbon monoxide reversibly binds to the deoxy form of tetrazole-Mb, and this complex was stable in sharp contrast to BrCN-MbCO, which was converted to the native MbCO with loss of the cyano group (Shiro & Morishima, 1984). The ^{1}H-NMR spectra showed that the ring current shifted Val E11 γ_1-methyl proton signal was observed at −6.86 and −7.15 ppm for tetrazole-MbCO and native MbCO, respectively (data not shown). The FT-IR spectra in the iron-ligated CO stretching region of native Mb and tetrazole-Mb are illustrated in Figure 5. The spectrum of native MbCO consists of mainly two distinguishable components for the iron-bound CO stretching frequencies, in which the most prominent absorption at 1945 cm^{-1} is characteristically observed (Figure 5A). On the other hand, the CO stretching band for tetrazole-Mb is observed at 1966 cm^{-1} as a single band (Figure 5B).

Laser Photolysis Measurements of CO Binding to Native Mb and Tetrazole-Mb. The CO association and dissociation rate constants, k_{on} (M^{-1} s^{-1}) and k_{off} (s^{-1}), and activation energies, ΔE_{on} (kcal/mol), for native Mb and tetrazole-Mb were obtained by laser photolysis measurements and are shown in Table I. The second-order association rate constants of CO binding to native Mb and tetrazole-Mb were determined by the CO-concentration dependence of the observed pseudo-first-order rate constants. The activation energies are obtained from the slope of the plot of ln k_{on} vs $1/T$. The modification of the distal His N-H to the *N*-tetrazole ring increased the CO-binding rate. The CO dissociation rate constant was also increased by the modification of the distal His.

DISCUSSION

A detailed analysis of ^{15}N-NMR spectra of tetrazole-Mb by using ^{15}N-labeled BrCN and N_3^- allowed us to reveal the mechanism of *N*-tetrazole ring formation at the distal histidyl imidazole in Mb; the distal histidyl *N*-CN group of BrCN-Mb reacts with N_3^- to form an *N*-tetrazolate ring by 1,3-cycloaddition, followed by rotational isomerization and binding of the nitrogen atom of the *N*-tetrazole ring to the ferric heme iron by the two binding modes to yield a novel hemichrome type of Mb derivative (Figure 3). In general, tetrazole derivatives are conveniently prepared from organonitriles via nucleophilic attack of the azide ion by a 1,3-dipolar cycloaddition reaction (Finnegan et al., 1958), and it is reasonable that the N-cyanated imidazole group of the distal histidine reacts with the external azide ion to form N-tetrazolated imidazole by the reaction scheme. Coordination of organoni-

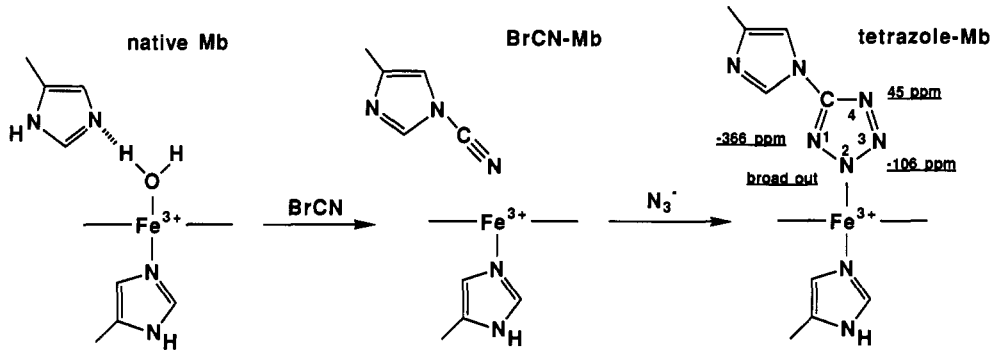

FIGURE 3: Heme environmental structures of ferric native Mb, BrCN-Mb, and tetrazole-Mb. Assignments of ^{15}N-NMR signals and the numbering order of the nitrogen atoms of the tetrazole ring are also shown. An anionic *N*-tetrazolate ring coordinates to the ferric heme iron of tetrazole-Mb at neutral pH (Kamiya et al., 1991).

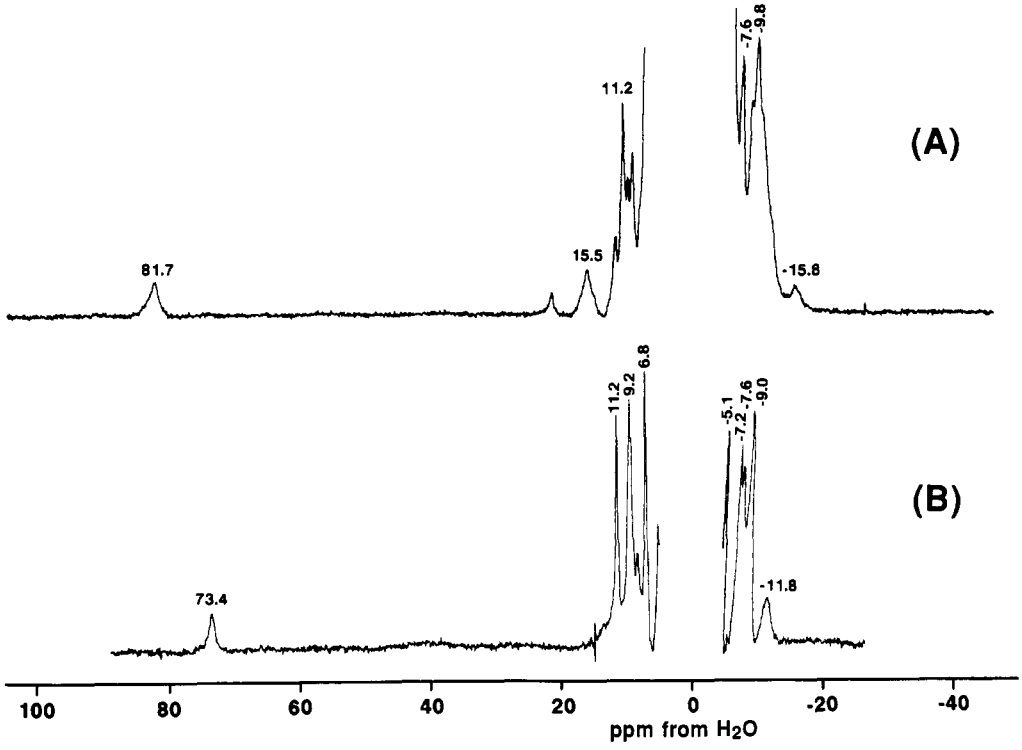

FIGURE 4: ^1H-NMR spectra of the deoxy forms of (A) tetrazole-Mb and (B) native Mb at pH 7 and 23 °C.

trile or azide to cobalt(III) or another metal is known to enhance this reaction (Ellis & Purcell, 1982; Erbe & Beck, 1983), but whether heme iron participates in this reaction is not obvious in the present stage.

Ferrous CO Derivative. The structural changes in the heme vicinity upon the modification are sensitively manifested in the ^1H-NMR spectra as the spectral shifts of the ring current shifted Val E11 γ_1-methyl proton resonance for a CO form. It has been well established that this resonance serves as a sensitive probe to monitor directly the conformational changes in the heme pocket. The Val E11 residue is located in the heme distal site situated next to the distal His as visualized by X-ray crystallographic study (Takano, 1977a,b), and its ^1H-NMR resonance position sensitively reflects the geometric relationship between the heme group and the Val E11 methyl group (Lindstorm et al., 1972; Lindstorm & Ho, 1973; Mims et al., 1983). The spectral shift of the Val E11 signal indicates the structural changes in the heme distal site upon the N-tetrazolation of the distal histidyl imidazole. According to the calculation made by Shulman et al. (1970), the downfield shift by 0.3 ppm of its signal implies that the methyl group of Val E11 moves up to 0.3 Å further away from the heme plane by the perturbation.

Further insight into the conformational changes in the heme vicinity was gained on the basis of the IR spectra of MbCO's as shown in Figure 5. It is well-known that, in sperm whale MbCO, mainly three structurally distinguishable components are involved with the IR absorptions at 1934, 1945, and 1967 cm^{-1} for the iron-bound CO stretching, and the configuration of the iron-bound CO for each C–O stretching frequency has been assigned. The difference in the C–O stretching frequency between the 1944- and the 1967-cm^{-1} conformer was interpreted in terms of the tilting angle of the C–O bond from the heme normal (Makinen et al., 1979; Chance et al., 1987; Moore et al., 1988; Ormos et al., 1988); the 1967-cm^{-1} conformer has upright binding geometry, while the 1944-cm^{-1} conformer bears relatively tilted geometry. This difference of the geometry of iron-bound CO has been interpreted that the 1967-cm^{-1} conformer corresponds to the "open" structure where ligand molecules readily enter into the heme pocket, whereas the 1944-cm^{-1} conformer is related to the "closed" structure where the entrance path for ligands is relatively blocked. As shown in Figure 5, N-tetrazolation of the distal

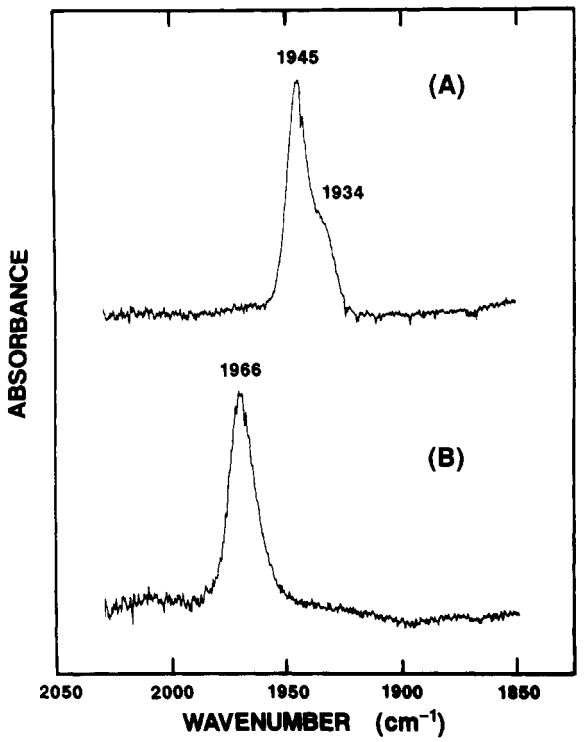

FIGURE 5: FT-IR spectra in the C–O stretching regions: (A) native MbCO, (B) tetrazole-MbCO.

Table I: Association and Dissociation Rate Constants of CO at 20 °C and Activation Energies for Association of CO for Native and Tetrazole-Mbs

	native Mb[a]	tetrazole-Mb[b]
k_{on} (M^{-1} s^{-1})	5.0×10^5	7.7×10^6
k_{off} (s^{-1})	0.015	0.1
ΔE_{on} (kcal/mol)	4.1	4.3

[a] Antonini and Brunori (1970). [b] This study.

histidyl imidazole increased the proportion of the 1967-cm^{-1} conformer. It is then reasonable that the 1967-cm^{-1} conformer is more favored than the 1944-cm^{-1} one, since the distal His is displaced farther away from the porphyrin ring by the N-tetrazolation. All the present FT-IR and ^{1}H-NMR spectra of tetrazole-MbCO suggest that the N-tetrazolation of the distal histidyl imidazole of Mb induces the structural changes in the heme vicinity; the amino acid residues in the heme distal site are forced to move further away from the heme plane and the structure of the heme pocket is relatively "open". The CO association rate constant for tetrazole-Mb also supports this assumption; the CO association rate constant was increased by 15-fold by *N*-tetrazole modification of the distal His (Table I). It is feasibly that the increase of the "open" conformer accelerates the CO rebinding rate. It is noteworthy that the increase of 1964-cm^{-1} conformer (the "open" conformer) and ca. 10-fold acceleration of the CO association rates are also observed for the distal His mutants (distal His → Gly or Met) of sperm whale Mb (Morikis et al., 1989; Rohlfs et al., 1990).

These results seem to contradict the simulation of rotation stability of the distal *N*-tetrazolyl His in tetrazole-Mb on the basis of the X-ray structure of ferric tetrazole-Mb and the ligand binding properties in its ferric state (Kamiya et al., 1991). In that study, some potential ligands of the ferric hemoproteins such as CN^-, N_3^-, F^-, and imidazole were found to be unable to bind to the tetrazole-Mb even at an acidic pH. (The tetrazole group dissociates from the ferric heme iron to form a pentacoordinate and high-spin state at an acidic pH.) These results were assumed to be due to the "closed" structure of the heme pocket of tetrazole-Mb. It is probable that the movement of the *N*-tetrazole ring is restricted by the electrostatic interaction with the positively-charged ferric heme iron, while such an interaction is negligible in the ferrous state due to the noncharged ferrous heme iron, and eventually, the *N*-tetrazole group can move further away from the heme plane.

Ferrous High-Spin State. As shown in Figure 4, the tetrazole-induced shift by 8.3 ppm for the proximal histidyl $N_\delta H$ for deoxy-Mb also significantly reflects the subtle perturbation at the heme proximity (Nagai et al., 1982; La Mar & de Ropp, 1982). Since the heme iron of deoxy-Mb has no sixth coordinated ligand (Takano, 1977b) and eventually has no direct interaction with the distal His, the substantial change of the $N_\delta H$ proton shift may result from the changes in the binding profiles of the proximal imidazole such as bond compression, tilting of the iron–imidazole bond, or modulation of the $N_\delta H$ hydrogen bonding. This suggests that the histidyl imidazole could occur in the heme distal site and to some extent in the proximal site as well.

Ferrous Oxy Derivative. *N*-Tetrazole modification of the distal histidyl imidazole altered the structure of Mb at the distal site and probably resulted in the inability of hydrogen bonding of the distal His with iron-bound O_2. The resultant effects may be manifested as the unique behaviors of the O_2 binding by the tetrazole-Mb. The lack of the hydrogen-bonding ability of the distal His in the modified Mb could be responsible for the present findings that ferrous tetrazole-Mb is readily oxidized rather than forms a stable oxy complex. It is to be noted that the recent study of the sperm whale Mb mutants (Springer et al., 1989) has shown that when the distal His is replaced by other residues such as Gly, Val, Tyr, etc., the rate of autoxidation is increased 40–350-fold, which would be due to a decrease in oxygen affinity and an increase in solvent anion accessibility to the distal pocket. A similar situation is supposed to be the case for tetrazole-Mb.

In conclusion, we have presented here the mechanism of *N*-tetrazole ring formation at the distal histidyl imidazole by ^{15}N-NMR spectroscopy utilizing ^{15}N-labeled BrCN and N_3^- and clarified the heme environmental structure and ligand binding properties of tetrazole-Mb in its ferrous state.

ACKNOWLEDGMENT

We are grateful to Dr. H. Masuda (Nagoya Institute of Technology), Dr. H. Hori (Osaka Univ.), and Drs. T. Iizuka, Y. Shiro, and N. Kamiya (The Institute of Physical and Chemical Research (RIKEN)) for their helpful discussion.

REFERENCES

Adachi, S., & Morishima, I. (1989) *J. Biol. Chem.* **264**, 18896–18901.

Antonini, E., & Brunori, M. (1970) *Hemoglobin and Myoglobin in Their Reactions with Ligands*, North-Holland, Amsterdam.

Carver, T. E., Rolhfs, R. J., Olson, J. S., Gibson, Q. H., Blackmore, R. S., Springer, B. A., & Sligar, S. G. (1990) *J. Biol. Chem. 265*, 20007–20020.

Chance, M. R., Campbell, B. F., Hoover, R., & Friedman, J. M. (1987) *J. Biol. Chem. 262*, 6959–6961.

Ellis, W. R., & Purcell, W. L. (1982) *Inorg. Chem. 21*, 834–837.

Erbe, J., & Beck, W. (1983) *Chem. Ber. 116*, 3867–3876.

Finnegan, W. G., Henry, R. A., & Lofquist, R. J. (1958) *J. Am. Chem. Soc. 80*, 3908–3911.

Hori, H., Fujii, M., Shiro, Y., Iizuka, T., Adachi, S., & Morishima, I. (1989) *J. Biol. Chem. 264*, 5715–5719.

Jajczay, F. L. (1970) Ph.D. Thesis, University of Alberta.
Kamiya, N., Shiro, Y., Iwata, T., Iizuka, T., & Iwasaki, H. (1991) *J. Am. Chem. Soc. 113*, 1826–1829.
La Mar, G. N., & de Ropp, J. S. (1982) *J. Am. Chem. Soc. 104*, 5203–5206.
Lindstorm, T. R., & Ho, C. (1973) *Biochemistry 12*, 134–139.
Lindstorm, T. R., Norem, I. B. E., Charache, S., Lehmann, H., & Ho, C. (1972) *Biochemistry 11*, 1677–1681.
Makinen, M. W., Houtchens, R. A., & Caughey, W. S. (1979) *Proc. Natl. Acad. Sci. U.S.A. 76*, 6042–6046.
McCoy, S., & Caughey, W. S. (1970) *Biochemistry 9*, 2387–2393.
Mims, M. P., Olson, J. S., Russu, I. M., Miura, S., Cedel, T. E., & Ho. C. (1983) *J. Biol. Chem. 258*, 6125–6134.
Moore, J. N., Hansen, P. A., & Hochsrtasser, R. M. (1988) *Proc. Natl. Acad. Sci. U.S.A. 85*, 5062–5066.
Morikis, D., Champion, P. M., Springer, B. A., & Sligar, S. G. (1989) *Biochemistry 28*, 4791–4800.
Morishima, I., Shiro, Y., Wakino, T. (1985) *J. Am. Chem. Soc. 107*, 1063–1064.
Morishima, I., Shiro, Y., Adachi, S., Yano, Y., & Orii, Y. (1989) *Biochemistry 28*, 7582–7586.
Nagai, K., La Mar, G. N., Jue, T., & Bunn, H. F. (1982) *Biochemistry 21*, 842–847.
Ormos, P., Braunstein, D., Frauenfelder, H., Hong, M. K., Lin, S.-L., Sauke, T. B., & Young, R. D. (1988) *Proc. Natl. Acad. Sci. U.S.A. 85*, 8492–8496.
Phillips, S. E. V., & Schoenborn, B. P. (1981) *Nature (London) 292*, 81–82.
Rohlfs, R. J., Mathews, A. J., Carver, T. E., Olson, J. S., Splinger, B. A., Egeberg, K. D., & Sligar, S. G. (1990) *J. Biol. Chem. 265*, 3168–3176.
Shiro, Y., & Morishima, I. (1984) *Biochemistry 23*, 4879–4884.
Shulman, R. G., Wuthrich, K., Yamane, T., Patel, D. J., & Blumberg, W. E. (1970) *J. Mol. Biol. 53*, 143–157.
Springer, B. A., Egeberg, K. O., Sligar, G. S., Rohlfs, R. J., Mathews, A. J., & Olson, J. S. (1989) *J. Biol. Chem. 264*, 3057–3060.
Takano, T. (1977a) *J. Mol. Biol. 110*, 537–568.
Takano, T. (1977b) *J. Mol. Biol. 110*, 569–584.
Witanowski, M., Stefaniak, L., & Webb, G. A. (1981) in *Annual Reports on NMR Spectroscopy* (Webb, G. A., Ed.) Vol. 11B, Academic Press, New York.

Registry No. His, 71-00-1; N_3^-, 14343-69-2; CO, 630-08-0; O_2, 7782-44-7; heme, 14875-96-8.